ELSEVIER

Chemical Engineering Journal 85 (2002) 225–234

Chemical Engineering Journal

www.elsevier.com/locate/cej

Heat and mass transfer in the evaporating film of a molecular evaporator

Juraj Lutišan [a], Ján Cvengroš [b,*], Miroslav Micov [b]

[a] *HighChem, Ltd., Jana Stanislava 35, 841 05 Bratislava, Slovak Republic*

[b] *Faculty of Chemical Technology, Slovak Technical University, Radlinského 9, 812 37 Bratislava, Slovak Republic*

Received 25 July 2000; received in revised form 28 February 2001; accepted 12 March 2001

Abstract

The hydrodynamic conditions in the wiped-film on the evaporating cylinder of a molecular evaporator have a considerable effect on the distillation output and composition of outlet streams from the evaporator. In this study, selected parameters are investigated in the laminar and turbulent regimes in the film, depending on the evaporator's liquid load and temperature. Results show that in the case of a turbulent film without concentration and temperature gradients at the same temperature of the evaporating cylinder surface, a higher portion of the feed is evaporated at a lower content of the more volatile component in the distillate. The model studied shows that there are only small differences in the relative volatility as a measure of separation efficiency in the turbulent or laminar film on the evaporating cylinder. The qualitative agreement between experimental results and the results from the model proposed shows that the model describes well the phenomena that occur within the distillation space of the molecular evaporator.

Keywords: Heat and mass transfer; Molecular distillation; Molecular evaporator; Wiped film; Relative volatility

1. Introduction

During molecular distillation in a short-path wiped-film evaporator, the distilled liquid continuously passes over the heated evaporating cylinder downward, partially evaporates and the vapours then condense on the cooled condenser placed close to the evaporating cylinder. A sufficiently low pressure, around 1 Pa, is reached in the evaporator. Therefore, evaporated molecules can pass through the distillation gap to the condenser without being disturbed. Gentle distillation of thermally unstable mixtures of liquids with low vapour pressure occurs with a theoretical rate of up to $40\,g\,m^{-2}\,s^{-1}$ practically without thermal decomposition at a reduced distillation temperature (lowered by 200–250 °C compared to that at normal pressure), with short residence times of the distilled liquid on the thermally exposed surface (about 10^{-1} to 10^{1} s), and at a small evaporating cylinder–condenser distance (20–50 mm).

The evaporation of the liquid on the evaporating cylinder is a key step in the molecular distillation. The distilled liquid flows over the cylinder as a thin wiped-film with a thickness of 0.05–2 mm according to the peripheral liquid load and the viscosity, while being evenly distributed around its perimeter and stirred by the action of the wiper. As a result of the intensive evaporation from the film surface without boiling, considerable concentration and temperature gradients are formed within the film. Thus, the content of the more volatile component in the film surface is decreased and the film surface is cooler compared to the average film temperature. The wiper function is to compensate such conditions, intensively mix the film and transport the heated lower layers rich in the more volatile component from the evaporating cylinder surface to the film surface. The real situation in the film is found somewhere between the two limit cases, i.e. between (a) the turbulent film with ideal mixing in the direction perpendicular to the flow without temperature and concentration gradients, and (b) the falling laminar film with a semi-parabolic velocity distribution and both temperature and concentration gradients. The design of wipers and wiping conditions substantially affects the film hydraulics on the evaporating cylinder [1].

It is natural that hydrodynamic conditions in the film manifest themselves in the output parameters, such as the quantity and composition of the distillate. In our preceding studies [2], we have created a complex mathematical molecular distillation model which describes the processes of the heat and mass transfer in the film of the evaporating liquid on the evaporating cylinder, the mass transfer in the distillation gap and also the heat and mass transfers in the condensed film on the condenser. The aim of this study is to evaluate differences between the laminar

* Corresponding author. Tel.: +421-7-59325-531; fax: +421-7-52493-198.
E-mail addresses: lutisan@highchem.com (J. Lutišan), cvengros@chtf.stuba.sk (J. Cvengroš).

1385-8947/02/$ – see front matter
PII: S1385-8947(01)00165-6

Nomenclature

c	molar concentration (mol m^{-3})
c_p	thermal capacity (J mol^{-1} K^{-1})
d	distance evaporator–condenser (m)
D	diffusion coefficient (m^2 s^{-1})
D/F	degree of evaporation
F	feed flow (mol s^{-1})
g	gravity (9.81 m s^{-2})
h	film thickness (m)
$\Delta_{evp}H$	heat of evaporation (J mol^{-1})
i	component A, B
I	flow (mol s^{-1})
j	surface: 1, evaporating cylinder; 2, condenser
k	evaporation rate (mol m^{-2} s^{-1})
k_{ij}	evaporation rate of the component i from surface j (mol m^{-2} s^{-1})
l	evaporator length (m)
M	molar weight (kg mol^{-1})
p^0	pressure of saturated vapour (Pa)
r	radius of the cylinder (m)
R	gas constant (8.314 J mol^{-1} K^{-1})
T	temperature (K)
T_{1W}	temperature of the evaporating cylinder wall (K)
T_{2W}	temperature of the condenser wall (K)
v	velocity (m s^{-1})
w	evaporation rate (mol m^{-1} s^{-1})
w_{ij}	evaporation rate of the component i from surface j (mol m^{-1} s^{-1})
W	residue (mol s^{-1})
x_F	mole fraction of more volatile component in the feed
x_W	mole fraction of more volatile component in the residue
X_1	mole fraction of more volatile component on the film surface on the evaporating cylinder
y	axis parallel to axis of the evaporator
z	axis perpendicular to axis of the evaporator

Greek letters

α	relative volatility
λ	thermal conductivity (W m^{-1} K^{-1})
ν	kinematics viscosity (m^2 s^{-1})
ρ	density (kg m^{-3})
Γ	peripheral liquid load (L dm^{-1} h^{-1})
Θ	total evaporation rate (mol m^{-2} s^{-1})
Ξ	coefficient of the resistance in the vapour phase
Ψ	coefficient of the splashing

and the turbulent regimes using the developed mathematical model of evaporation from the liquid film surface at high vacuum and to appreciate the effect of wiping intensity on the evaporator's output and separation efficiency.

Several studies report the results of modelling the molecular distillation process. Bose and Palmer [3] have given reasons for a separation efficiency decrease by distillation in a jet tenzimeter. This decrease is caused by both concentration and temperature gradients in the distilled liquid mixture as a consequence of intense evaporation. Kawala and Stephan [4] have simulated the processes in falling-film with an adiabatic regime. Ferron and Bhandarkar [5] have presented a description of heat and mass transfer in liquid film on the conical evaporator of a centrifugal still. Batistella and Maciel [6] have compared, in model terms, the performance and efficiency of the falling-film and centrifugal distillators, respectively. Toei et al. [7] have studied the influence of the inert gas pressure on the process of molecular distillation. Nguyen and Goffic [8] have developed a model of wiped-film molecular evaporator. We have used our developed model for modelling various design and operating situations in a molecular evaporator, such as the fractionation in the evaporator with a divided condenser [9], the influence of feed temperature on the evaporator performance [10], the effect of an adiabatic separator in the distillation gap on the separation efficiency [11] and the effect of inert gas pressure on the molecular distillation process [12]. The mean free path of the molecules was studied using the DSMC method in [13].

2. Mathematical description of the problem

An apparatus for falling-film molecular distillation is shown in Fig. 1. It consists of a cylindrical evaporator surrounded by a condenser jacket. The liquid to be distilled is transported on the evaporating surface. There it flows down in the form of a film and is partly vaporised. The evaporating cylinder is heated internally by the heating fluid with constant temperature T_{1W}. Evaporated molecules condense on the closely positioned condenser. The condensing cylinder

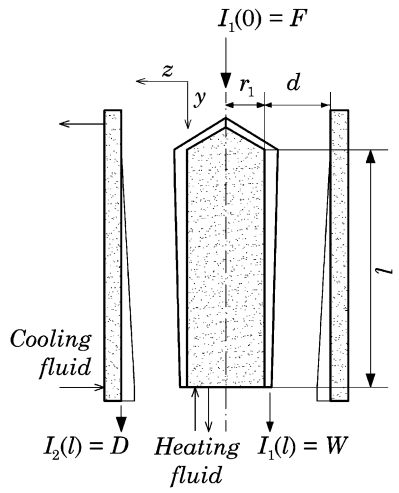

Fig. 1. Scheme of the falling-film molecular evaporator.

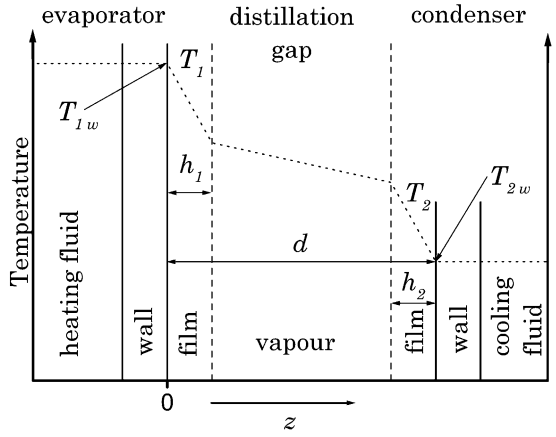

Fig. 2. Temperature profile in the molecular evaporator.

is cooled by the cooling fluid with constant temperature T_{2W}. If both films are much thinner than the evaporating cylinder and condenser diameters, the liquid films can be regarded as planar. The temperature profile in the molecular evaporator is shown in Fig. 2.

The assumption that the distilled liquid consists of two components *A*, *B* will be used in our work.

The relation describing the flow I_1 on the evaporating cylinder is given by the continuity equation

$$\partial_y I_{i1}(y) = -2\pi r_1 X_{i1} k_{i1} + 2\pi r_2 X_{i2} k_{i2} \tag{1}$$

where

$$k_{ij} = \frac{X_{ij} p_i^0(T_j)}{\sqrt{2\pi R M_i T_j(y, h_j)}} \tag{2}$$

and where $i = A$ (component *A*) or *B* (component *B*) and $j = 1$ (evaporating cylinder) or 2 (condenser).

The initial condition is

$$I_1(0) = F = \frac{2\pi r_1 \Gamma \rho}{3.6 \times 10^5 M}, \qquad I_2(0) = 0 \tag{3}$$

The parameters for heat and mass transfers under steady-state conditions are described by four fundamental balance equations:

- Boltzmann equation for mass transfer in the vapour phase. If the pressure in the distillation gap is very low, the vapour phase does not influence the process and Boltzmann equation can be omitted.
- Navier–Stokes equation for film flow in the falling-film.
- Equation for diffusion.
- Thermal balance equation.

The Navier–Stokes equation of liquid flow in the falling-film is formulated as

$$(\vec{v}_j \operatorname{grad} \vec{v}_j) = \nu \nabla^2 \vec{v}_j + \vec{g} \tag{4}$$

In the case of the molecular evaporator, the Nusslet's solution of Eq. (4) is sufficient. So, for the value of velocity component in the direction of the *y*-axis on the surface *j* (see Fig. 1) the expression is governed by

$$v_{yj}(y, z) = \frac{g h_j^2}{\nu} \left[\frac{z}{h_j} - \frac{1}{2} \left(\frac{z}{h_j} \right)^2 \right] \tag{5}$$

The equation of diffusion has the general form:

$$\operatorname{div}(\vec{v}_j c_{ij}) = \operatorname{div}(D_i \operatorname{grad} c_{ij}) \tag{6}$$

Diffusion coefficient D_i is to be held constant.

The boundary conditions between the film and vapour are determined by the Langmuir–Knudsen relation for the rate of evaporation:

$$w_{ij} = 2\pi r_j X_{ij} k_{ij} = \frac{2\pi r_j X_{ij}(y, h_j) p_i^0(T_j)}{\sqrt{2\pi R M_i T_j(y, h_j)}} \tag{7}$$

The relation (7) describes the evaporation rate of component *i* from the film *j*.

If the influence of collisions between the molecules in the vapour phase is neglected, it is possible to describe the total evaporation rate in the form

$$\begin{aligned} \Theta_{i1} &= w_{i1} - w_{i2} = \frac{2\pi r_1 X_{i1} p_i^0(T_1)}{\sqrt{2\pi R M_i T_1}} - \frac{2\pi r_2 X_{i2} p_i^0(T_2)}{\sqrt{2\pi R M_i T_2}}, \\ \Theta_{i2} &= w_{i2} - w_{i1} = \frac{2\pi r_2 X_{i2} p_i^0(T_2)}{\sqrt{2\pi R M_i T_2}} - \frac{2\pi r_1 X_{i1} p_i^0(T_1)}{\sqrt{2\pi R M_i T_1}} \end{aligned} \tag{8}$$

The thermal balance equation can be expressed in the form

$$c_p \operatorname{div}(\vec{v}_1 T_1) = \operatorname{div}(\lambda \operatorname{grad} T_1) \tag{9}$$

Thermal conductivity λ and thermal capacity c_p are regarded as constants.

The boundary conditions for Eq. (9) between the film and the vapour phase can be then formulated as

$$\begin{aligned} \lambda \left. \frac{\partial T_1}{\partial z} \right|_{z=h_1} &= -\sum_{i=A}^{B} \Delta H_i \times \left(\frac{2\pi r_1 X_{i1} p_i^0(T_1)}{\sqrt{2\pi R M_i T_1}} - \frac{2\pi r_2 X_{i2} p_i^0(T_2)}{\sqrt{2\pi R M_i T_2}} \right), \\ \lambda \left. \frac{\partial T_2}{\partial z} \right|_{z=h_2} &= -\sum_{i=A}^{B} \Delta H_i \times \left(\frac{2\pi r_2 X_{i2} p_i^0(T_2)}{\sqrt{2\pi R M_i T_2}} - \frac{2\pi r_1 X_{i1} p_i^0(T_1)}{\sqrt{2\pi R M_i T_1}} \right) \end{aligned} \tag{10}$$

3. Solution of the balance equations

The solution of equations describing diffusion and thermal balance is a crucial problem and it is described in our previous publication [2].

The first used assumption is a quadratic profile of concentration of the more volatile component in the film:

$$X_{A1} = \frac{\mathcal{D}_j x_{Aj}}{\mathcal{D}_j + \Delta k_1} \tag{11}$$

$$X_{A2} = \frac{a_1 - \sqrt{a_2}}{2\Delta k_2} - 3\left(\frac{a_1 - \sqrt{a_2}}{2\Delta k_2} - x_{A2}\right) \tag{12}$$

where

$$\mathcal{D}_j = \frac{4D_j c_j}{h_j}$$

$$a_1 = \mathcal{D}_2 + \Delta k_2 - \Delta k_1 X_{A1} - k_{B1}$$

$$a_2 = a_1^2 - 4\Delta k_2 \mathcal{D}_2 x_{A2}$$

$$\Delta k_i = k_{Ai} - k_{Bi}$$

Finally, substituting X_{A1} from the Eq. (11) and X_{A2} from the Eq. (12) in Eq. (1), we obtain the set of the balanced equations.

Parameter k_{ij} from Eq. (1) depends on the surface temperatures of the films $T_j(h_j)$. These temperatures will be determined from boundary condition (10) using the assumption that the profile of the temperature in the film is linear. Accepting this as a new form of thermal boundary conditions, we obtain for the evaporating cylinder and for the condenser:

$$\lambda\frac{T_1(y,h_1) - T_{1W}}{h_1} = -\sum_{i=A}^{B}\Delta H_i\left(\frac{2\pi r_1 X_{i1} p_i^0(T_1)}{\sqrt{2\pi R M_i T_1}} - \frac{2\pi r_2 X_{i2} p_i^0(T_2)}{\sqrt{2\pi R M_i T_2}}\right),$$

$$\lambda\frac{T_2(y,d-h_2) - T_{2W}}{h_2} = -\sum_{i=A}^{B}\Delta H_i\left(\frac{2\pi r_2 X_{i2} p_i^0(T_2)}{\sqrt{2\pi R M_i T_2}} - \frac{2\pi r_1 X_{i1} p_i^0(T_1)}{\sqrt{2\pi R M_i T_1}}\right) \tag{13}$$

So, the process of the evaporation is fully described by the differential Eq. (1) for $i = A$, B and $j = 1$, surface molar fraction described by Eqs. (11) and (12) and by the set of boundary conditions described by Eq. (13).

4. Influence of the vapour phase resistance and splashing

In a real situation, involving vapour transfer through the distillation space, intermolecular collisions occur. This results in the return of part of the vapour back to the evaporating surface. Assuming that the re-evaporation from the condenser does not occur, the "permeability" of the distillation space can be expressed by the factor Ξ as a coefficient of a resistance in the vapour phase

$$\partial_y I_{i1}(y) = -2\pi r_1 k_{i1} X_{i1} \Xi_i \tag{14}$$

where Ξ has value zero if all evaporated molecules return back to the evaporation surface and value one, if all evaporated molecules condense on the condenser (ideal state).

Also, in a real situation, after the feed enters the evaporation surface, intensive escape of the volatile components and dissolved gases arises. These components also bear a part of the distilled liquid in the form of small droplets, deteriorating the distillate. This phenomenon is called splashing. It can be incorporated in the model by the factor Ψ as a coefficient of splashing in Eq. (15):

$$\partial_y I_{i1}(y) = -2\pi r_1 X_{i1} k_{i1} - 2\pi r_1 \Psi \sum_{n=A}^{B}(k_{n1} x_{n1}) \tag{15}$$

The factor Ψ can reach the value zero when the splashing does not occur, or some other positive value up to one which shows the part of the liquid flowing downwards on the evaporating surface which is transported to the condenser as splashing. Its numerical value is related to the evaporation rate on a given area of the evaporating surface.

By taking into account both, the resistance in the vapour phase and the splashing, the balance equation for the mass transfer through the evaporation space takes the form:

$$\partial_y I_{i1}(y) = -2\pi r_1 k_{i1} \Xi - 2\pi r_1 \Psi \sum_{n=A}^{B}(k_{n1} x_{n1}) \tag{16}$$

5. Results and discussion

For simulation, two evaporator peripheral liquid loads Γ of 5 and 7 l dm^{-1} h^{-1} of a binary mixture of di-(ethylhexyl)-phthalate (EHP) and di-(2-ethylhexyl)sebacate (EHS) with a mole fraction of the more volatile component $x_{EHP} = 0.500$ were considered at two different evaporating cylinder wall temperatures, 433 and 453 K, within the laminar and turbulent regimes on the evaporating cylinder. The film on the condenser is always assumed to be in the laminar regime. For the calculations, the following physical values were used.

For EHP ($M = 0.391$ kg mol^{-1}): $\Delta_{evp}H = 104.82$ kJ mol^{-1}, $\rho(100^\circ\text{C}) = 983$ kg m^{-3}, $\lambda = 3.58 \times 10^8 c_p M\rho(\rho/1000M)^{1/3}$, $\log\nu = -14.34709 + 8234.31/T - 2.88236 \times 10^6/T^2 + 3.95358 \times 10^8/T^3$, $c_p = 612$ J K^{-1} mol^{-1} (Neumann–Kopp), $\ln p^0 = 32.003 - 12658/T$ Pa. For EHS ($M = 0.421$ kg mol^{-1}): $\Delta_{evp}H = 110.35$ kJ mol^{-1}, $\rho(100^\circ\text{C}) = 912$ kg m^{-3}, $\log\nu = -7.45339 + 1213.95221/T - 421818.97765/T^2 + 9.06023 \times 10^7/T^3$, $c_p = 742$ J K^{-1} mol^{-1} (Neumann–Kopp), $\ln p^0 = 31.635 - 13056/T$ Pa. Diffusion coefficients were determined by the Reddy and Doraiswamy method [14].

Furthermore, it is presumed that the effect of collisions in the distillation gap is negligible. The modelled molecular evaporator has a 30 mm-diameter evaporating cylinder with an evaporating cylinder–condenser distance of 10 mm.

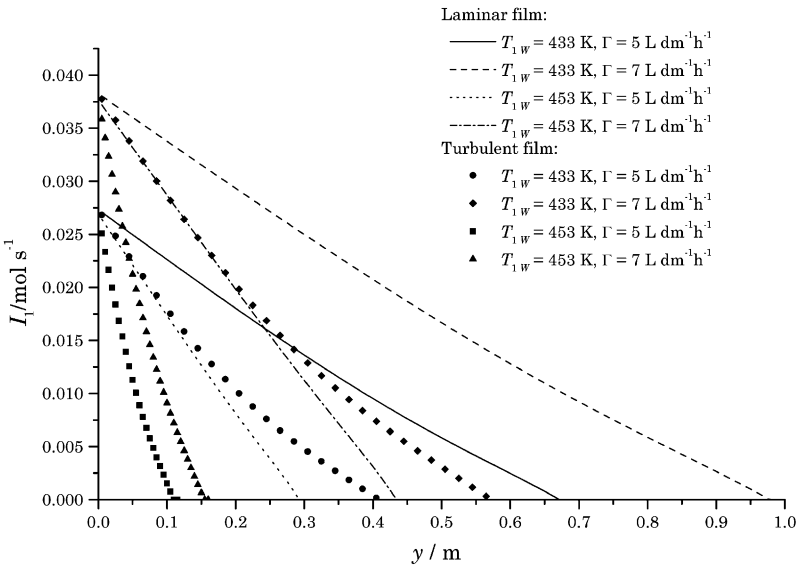

Fig. 3. Dependence of the liquid flow on the evaporating cylinder height for laminar and turbulent regimes.

Fig. 3, shows the values of liquid flows at different heights of the evaporating cylinder for the laminar and turbulent regimes in the film at the two cylinder surface temperatures and the two liquid loads Γ. There are two sets of curves, each starts from the point corresponding to its respective liquid load. The flow intensity in the turbulent regime is changing more vigorously than in the laminar regime. This difference is caused, primarily, by a higher surface film temperature in the turbulent regime, where this temperature is equal to the temperature of evaporating cylinder wall. For this reason, the degree of evaporation, expressed as a ratio of the distillate weight to the feed, is considerably higher in the turbulent regime (Fig. 4).

There is a temperature gradient in the laminar film on the evaporating cylinder, which, however, is not present in the turbulent film. This is shown in Fig. 5, which displays the dependence of the film surface temperature on the evaporating cylinder height. This gradient causes the film surface temperature to be lower and, thus, the evaporation therefore occurs at a reduced rate. This results in a lower evaporation degree mentioned above according to Fig. 4 and in higher value of the liquid flow shown in Fig. 3.

Fig. 6 displays the film thickness in various heights of the evaporating cylinder. The thickness of the film decreases considerably quickly in the turbulent regime as a result of the higher degree of evaporation and a lower film viscosity at the increased film temperature.

Fig. 7 shows the surface composition of a liquid on the evaporating cylinder, where the tendencies mentioned above remained unchanged; the content of the more-volatile com-

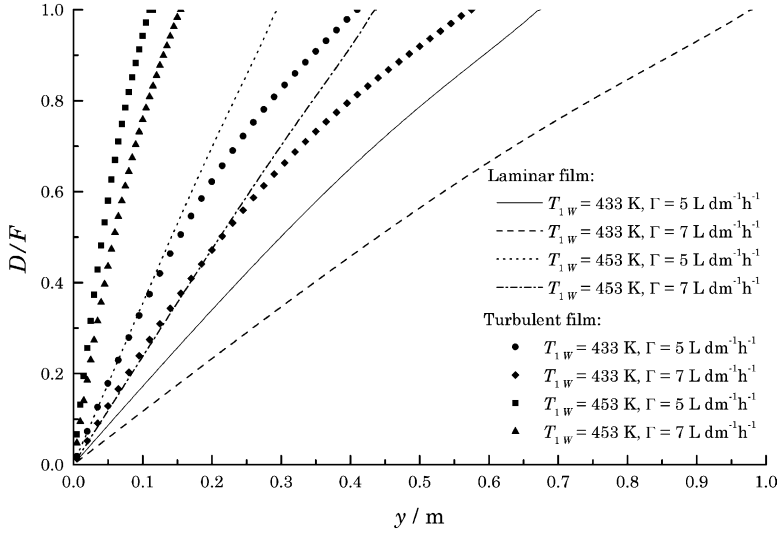

Fig. 4. Dependence of the evaporation degree on the evaporating cylinder height for laminar and turbulent regimes.

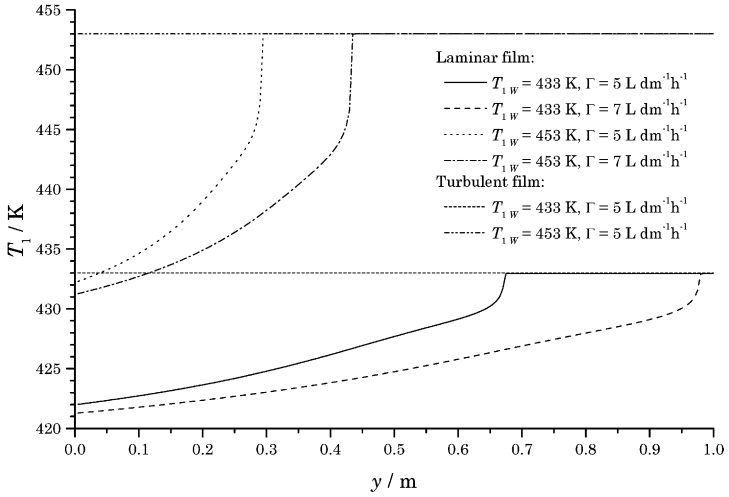

Fig. 5. Dependence of the surface temperature of laminar film on the evaporating cylinder height.

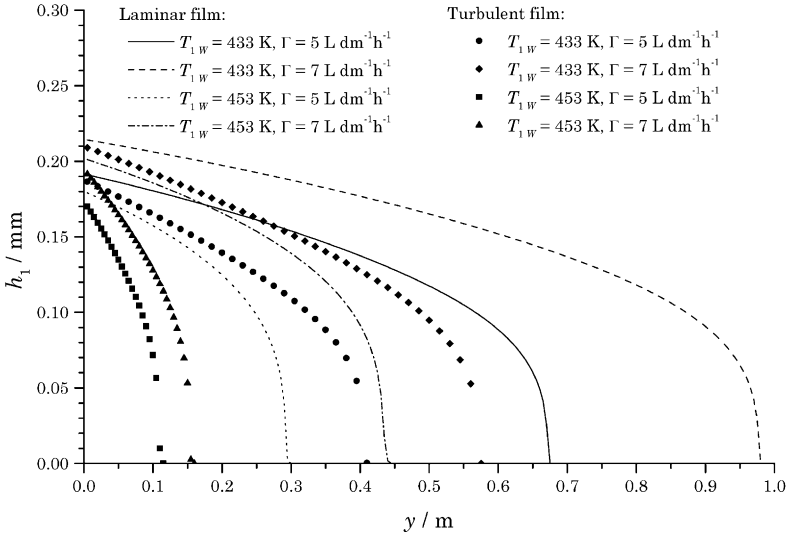

Fig. 6. Dependence of the film thickness on the evaporating cylinder height for laminar and turbulent regimes.

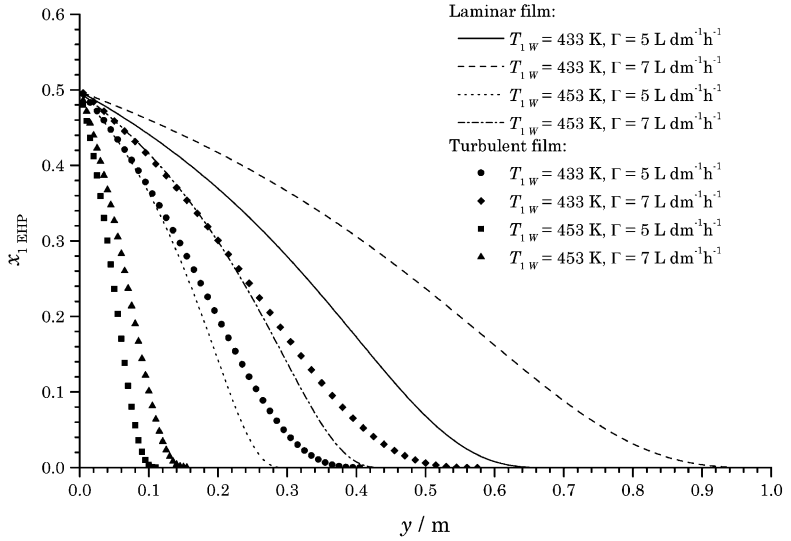

Fig. 7. Dependence of the film surface composition on the evaporating cylinder height for laminar and turbulent regimes.

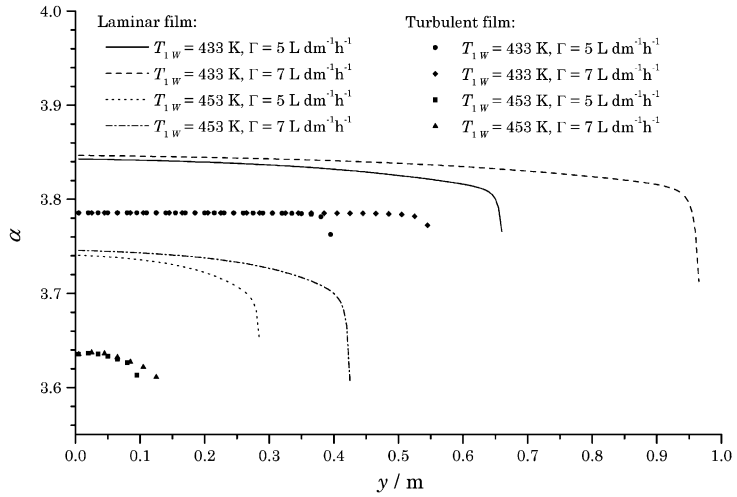

Fig. 8. Dependence of the relative volatility on the evaporating cylinder height for laminar and turbulent regimes.

ponent in the film surface decreases more markedly in the turbulent regime.

In the case of distillation on continuous film evaporators, the Rayleigh equation is usually used for determining the separation efficiency of the process which is expressed by the relative volatility α:

$$\alpha = 1 + \frac{\ln\{x_W(1-x_F)/[x_F(1-x_W)]\}}{\ln\{W(1-x_W)/[F(1-x_F)]\}} \tag{17}$$

where $F = I_1(0)$, $W = I_1(l)$, $x_F = I_{A1}(0)/I_1(0)$, $x_W = I_{A1}(l)/I_1(l)$.

The theoretical value of separation efficiency for molecular distillation is defined by Eq. (18):

$$\alpha_T = \frac{k_{A1}}{k_{B1}} = \frac{p_A^0}{p_B^0}\sqrt{\frac{M_B}{M_A}} \tag{18}$$

In Fig. 8, are shown functions $\alpha = f(y)$ for the operating parameters studied. According to the theory, the relative volatility in the turbulent regime has a constant value consistent with Eq. (18). For higher temperatures, the value of α is lower. The initial value of α is higher in the laminar film compared to the turbulent film as a result of the lower film surface temperature. The film surface temperature increases with the degree of evaporation, thus, causing a moderate decrease in the value of α. The individual curves end at a point, where the film on the evaporating cylinder is completely evaporated.

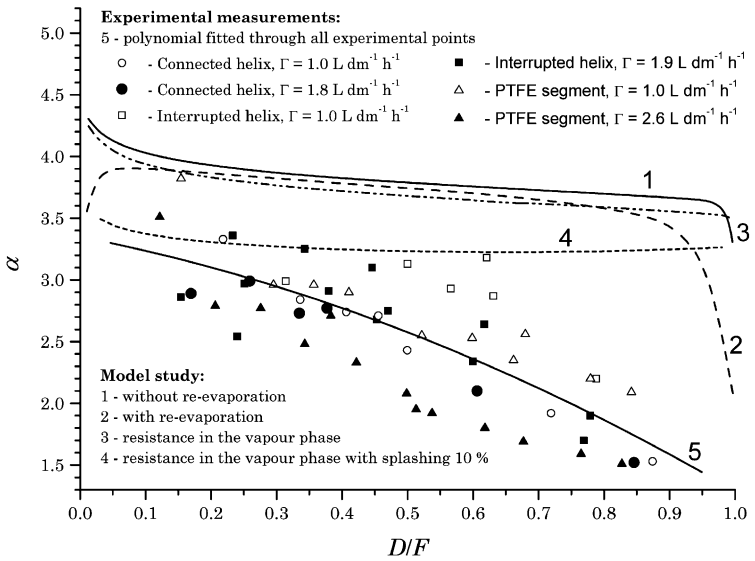

Fig. 9. Dependence of the relative volatility on the evaporation degree for different distillation modes. Laminar film: $T_{1W} = 433$ K, $T_{2W} = 293$ K (curve 1, 3–5), 353 K (curve 2).

In Fig. 9, are curves showing the dependence of the relative volatility, α on the degree of evaporation (D/F) computed from Eq. (17) for an evaporator of a 30 mm diameter with a final length of 300 mm for some, selected, model situations. Such a computed value of the relative volatility provides complex information on the separation within the evaporator under real conditions when a substantial portion of the feed has evaporated. The separation efficiency, which is worse than the theoretical one, is related either to the theoretical distillate composition at its smaller amount, or the distillate composition has deteriorated, compared to theory, at the theoretical amount of the distillate. In practice, the deterioration in separation efficiency is caused by lower values of both of these parameters compared to the theoretical ones.

In all cases, there is a laminar film on the evaporator, evaporating cylinder wall temperature $T_{1W} = 433\,\mathrm{K}$, liquid load $\Gamma = 7\,\mathrm{L\,dm^{-1}\,h^{-1}}$ and laminar film on condenser.

In our previous studies, the resistance to the mass transfer in the vapour phase was neglected in our model. The shape of function $\alpha = f(D/F)$ for this simplest case without re-evaporation is described by curve 1 in Fig. 9. On the evaporator's condenser, a certain re-evaporation of condensed molecules always occurs, depending on the actual temperature what is expressed by Eq. (7). Providing that the condenser wall temperature $T_{2W} = 353\,\mathrm{K}$, what represents real distillation conditions, it is possible to evaluate this phenomenon for the EHP–EHS testing mixture used that results in curve 2 in Fig. 9. By comparing these two curves, it is evident that the re-evaporation has a small effect on the separation efficiency under the given conditions.

In the vapour phase, however, other processes take place. Their effect has not yet been included into the model. Our study on the evaporation in molecular evaporator using the DSMC method [11–13] showed that there are complicated conditions existing just above the evaporating surface. This leads to the return of a portion of the already evaporated molecules back onto the evaporating surface. In addition, splashing comes into play in a real distillation. This means a mechanical transfer of microscopic droplets of the liquid from the evaporating cylinder onto the condenser that can be caused, e.g. by insufficient degassing. The above mentioned flows are shown schematically in Fig. 10. It is necessary to assess to what extent they can affect the separation efficiency. When evaluating the resistance of the vapour phase using the DSMC method, the coefficient Ξ dependent on temperature is determined. This coefficient is equal to zero if all of the evaporated molecules are captured in the vapour phase or is equal to one if the vapour phase has no resistance. Taking this into account, curve 3 in Fig. 9 was obtained for the case of a resistance in the vapour phase with no splashing, while a resistance in the vapour phase with a 10% splashing was considered to calculate curve 4.

The factor Ξ in Eq. (14) was calculated by the DSMC method as the dependence on the surface temperature T_1 and the surface composition on the evaporation cylinder $X_{i\,1}$. Splashing factor Ψ was fixed at $\Psi = 0.1$.

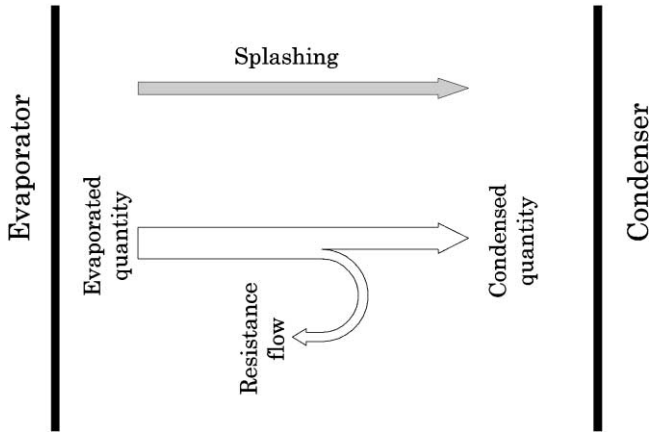

Fig. 10. Scheme of flows in the distillation gap of the molecular evaporator.

Both the processes reduce the separation efficiency. The decrease is not significant in the case of the resistance of the vapour phase, but is already greater in the case of splashing and the vapour resistance. The relative volatility maintains values mostly independent of the D/F parameter in all the specified model situations.

Included in Fig. 9 are 55 experimental values of the relative volatility α calculated from Eq. (17) for different values of the evaporation degree, D/F, for two feed rates and with three types of wipers: connected helix [15] (Fig. 11a), interrupted helix [15] (Fig. 11b), and PTFE segment wiper [16] (Fig. 11c). In all cases, the diameter of the evaporating cylinder and its length are the same as at the model study, 30 and 300 mm, respectively. Line 5 in Fig. 9 is a polynomial fitted by regression analysis through all the experimental points. The peripheral speed of the wipers was small, about $5\,\mathrm{m\,min^{-1}}$, so the laminar regime remains conserved.

The experimental values of α show a greater dependence on the evaporation degree than do the values from the model study. There is an evident drop in the experimental relative volatility at higher evaporation degrees [17]. It seems that at higher evaporation degrees there are additional factors which decrease the relative volatility which are not satisfactorily accounted for within the model, however, in general, the model qualitatively describes the real situation in the evaporator especially after the inclusion of splashing.

Fig. 12 shows profiles of the condensate surface temperature on the condenser. Only the laminar regime is supposed there. This corresponds to the real conditions in molecular

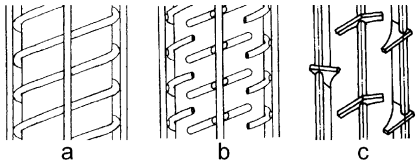

Fig. 11. The types of wiper used in the experimental study of relative volatility (a) connected metal helix, (b) interrupted metal helix with protecting PTFE tubes, (c) PTFE segment wiper.

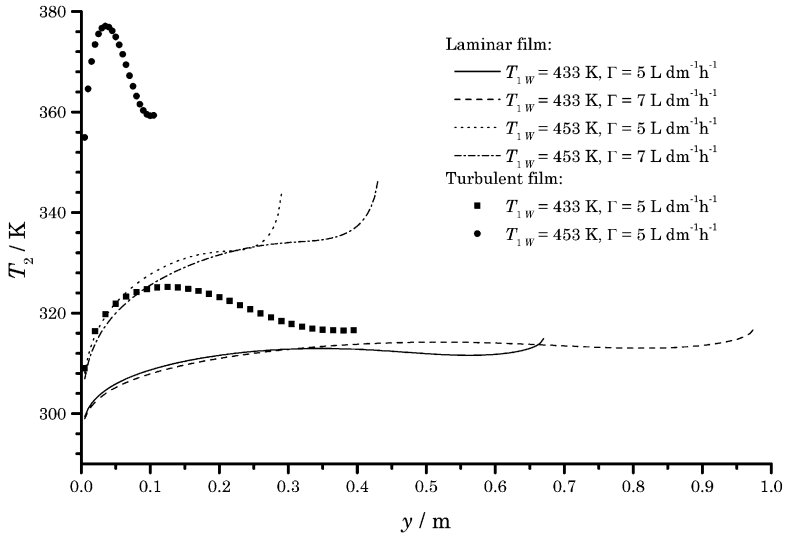

Fig. 12. Dependence of the condenser film surface temperature on the evaporating cylinder height for laminar and turbulent regimes.

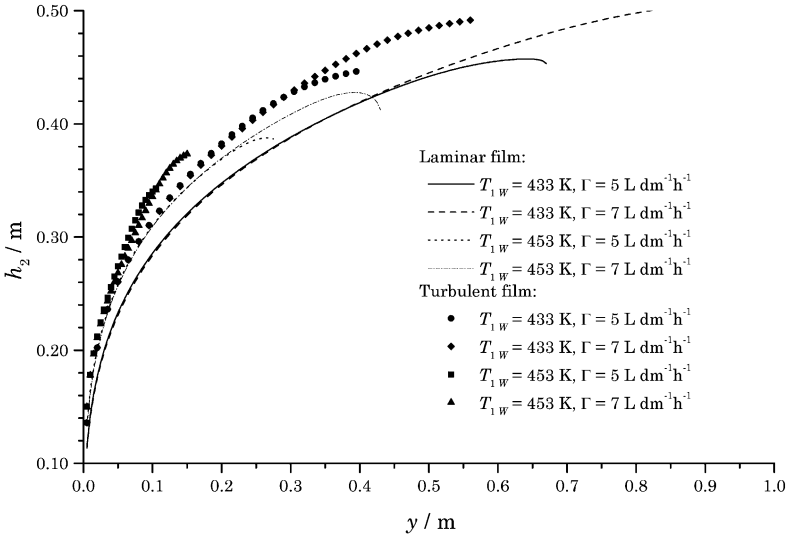

Fig. 13. Dependence of the condenser film thickness on the evaporating cylinder height for laminar and turbulent regimes at the evaporating cylinder.

distillation when the condenser is not wiped. The film of the condensate is formed evenly along the whole condenser perimeter. Individual curves then correspond to the situation on the evaporating cylinder. The elevated film surface temperature as well as the increased film thickness on the condenser (Fig. 13) are a logical consequence of the increased flow of the liquid on the condenser under more advantageous conditions on the evaporating cylinder (higher temperature, turbulent regime).

6. Conclusion

The model studying hydrodynamic regimes in a liquid film on the evaporating cylinder of a molecular evaporator showed that the distillation rate in the turbulent regime is much higher than in the laminar regime at the same surface temperature of the evaporating cylinder. The higher evaporation output for the same time of exposure of a heat-sensitive substance to the effect of elevated temperature decreases the risk of thermal decomposition. The effect of both investigated regimes on the evaporator separation efficiency is small. Comparison of the experimental values of relative volatility with values from the model show good qualitative agreement between experiment and model.

Acknowledgements

This work was partially supported by Slovak Grand Agency for Science, Project no. 1/5210/98.

References

[1] J. Cvengroš, Š. Pollák, J. Lutišan, Chem. Eng. Technol. 23 (2000) 55.
[2] M. Micov, J. Lutišan, J. Cvengroš, Sep. Sci. Technol. 32 (1997) 3051.
[3] A. Bose, H.J. Palmer, Ind. Eng. Chem. Fundam. 23 (1984) 459.
[4] Z. Kawala, K. Stephan, Chem. Eng. Technol. 12 (1989) 406.
[5] J.R. Ferron, M. Bhandarkar, Ind. Eng. Chem. Res. 29 (1991) 998.
[6] C.B. Batistella, M.R.W. Maciel, Comp. Chem. Eng. 20 (Suppl.) (1996) S19.
[7] R. Toei, M. Okazaki, M. Asaeda, J. Chem. Eng. Jpn. 4 (1971) 188.
[8] A.N. Nguyen, F. Le Goffic, Chem. Eng. Sci. 52 (1997) 2661.
[9] J. Cvengroš, M. Micov, J. Lutišan, Chem. Eng. Processing 39 (2000) 191.
[10] J. Cvengroš, J. Lutišan, M. Micov, Chem. Eng. J. 78 (2000) 61.
[11] J. Lutišan, M. Micov, J. Cvengroš, Sep. Sci. Technol. 33 (1998) 83.
[12] J. Lutišan, J. Cvengroš, Sep. Sci. Technol. 30 (1995) 3379.
[13] J. Lutišan, J. Cvengroš, Chem. Eng. J. 56 (1995) 39.
[14] K.A. Reddy, L.K. Doraiswamy, Ind. Eng. Chem. Fundam. 6 (1967) 77.
[15] A. Tkáč, J. Cvengroš, Ind. Eng. Chem. Process Des. Develop. 17 (1978) 242.
[16] J. Cvengroš, V. Badin, Š. Pollák, Chem. Eng. J. 59 (1995) 259.
[17] J. Cvengroš, A. Tkáč, Ind. Eng. Chem. Process Des. Develop. 17 (1978) 246.